Macromolecules

ARTICLE

pubs.acs.org/Macromolecules

Influence of Charged Polymer Coatings on Electro-Osmotic Flow: Molecular Dynamics Simulations

Owen A. Hickey,[†,‡] Christian Holm,[†] James L. Harden,[‡] and Gary W. Slater*[,‡]

[†]Institute for Computational Physics, Universität Stuttgart, Pfaffenwaldring 27, 70569 Stuttgart, Germany

[‡]Department of Physics, University of Ottawa, 150 Louis-Pasteur, Ottawa, Ontario K1N 6N5, Canada

ABSTRACT: Electro-osmotic flow (EOF) plays a crucial role in the functioning of devices in micro- and nanofluidics. In order to optimize the operation of a device, polymer coatings are often used to control EOF. Our simulations examine the case of grafted, charged polymer coatings for this purpose and compare the electro-osmotic flow mobility produced by a given polymer coating to the free-flow electrophoretic mobility of the polymers making up that coating. The simulation results are compared to both experimental data and theoretical predictions. One particularly interesting result is that the direction of the EOF reverses well before the net charge of the interface changes sign.

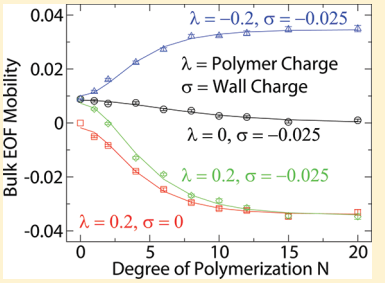

I. INTRODUCTION

In micro- and nanofluidic devices surfaces frequently become charged when placed in contact with an aqueous buffer. This process creates a thin oppositely charged layer of mobile fluid next to the surface, called the Debye layer. When an electric field is applied parallel to the surface, this thin layer of fluid generates a pluglike flow outside the Debye layer called electro-osmotic flow (EOF). In the case of capillary electrophoresis, EOF increases dispersion in the system (thereby reducing resolution) due to the nonuniform character of the flow resulting from unavoidable heterogeneity in the surface charge of capillaries.[1] For this reason scientists have long sought to suppress EOF by making use of polymer coatings in capillary electrophoresis.[2,3] In other situations, however, some EOF can actually be beneficial to the functioning of the system.[4] For example, in many microfluidic devices, EOF is used as a pump to move chemicals and samples.[5] In such cases it might be desirable to maximize EOF while keeping it as uniform as possible.[6] Our interest here is the role of a charged polymer coating for the control of EOF in the context of capillary electrophoresis and other electro-osmotic microfluidic systems.

Recent computer simulations have probed the role of neutral grafted polymer coatings in modulating EOF.[7−12] The simulations of Tessier and Slater[7,8] provided the first computational evidence for the scaling predictions of Harden et al.[13] for the effect of the length and grafting density of the polymers in the coating. Qiao has investigated the role of the electric field[10] as well as the role of physicochemical interactions on scales smaller than the Debye length.[9] Cao et al. studied how solvent quality changes the struture of polymer coatings and how this in turn affects EOF.[11,12] Our group has also made use of coarse-grained molecular dynamics simulations in order to look at the role of dynamically adsorbed polymer coatings in the modulation of EOF.[14] These simulations were able to qualitatively reproduce the experimental results of Doherty et al.[15]

The relationship between polymer coatings and EOF in a tube is rather complex, as the structure of the layer and the flow through the layer are intimately related. This is particularly true in the nonlinear regime of flows that are sufficiently strong to deform the polymer conformations in the layer. In principle, the conformation of polymers and the EOF profile in the layer can be determined self-consistently for simplified models, but often important phenomena are ignored in such theoretical and computational studies. For instance, many studies neglect hydrodynamic interactions in the polymer layer. However, recent studies have shown that such a free-draining approximation is not generally valid, particularly when the Debye length is comparable to or smaller than the thickness of the layer.[16] In fact, the force needed to hold a grafted polyelectrolyte still in an electric field is proportional to its hydrodynamic radius and not the total charge on the polymer in the limit of thin Debye layers,[17,18] a direct reflection of the effective hydrodynamic drag on the polymer due to EOF. Another intriguing effect that has received some attention in recent years is the role of the relative distribution of charge between the bare surface and the polymer layer on the resulting EOF.[9,11,14]

In this article, we present coarse-grained molecular dynamics (MD) simulation studies of the role of charged, grafted polymer coatings on EOF, highlighting several fascinating phenomena. First, results are presented showing that the EOF reverses direction before the net charge of the interface (the wall together with the grafted polymers) changes sign. Next, we compare simulation results to the predictions of Harden et al.[13] and find

Received: August 31, 2011
Revised: October 24, 2011
Published: November 16, 2011

good agreement with their scaling predictions. We also test the hypothesis that for relatively thick polymer coatings the EOF is expected to be of equal magnitude but opposite sign to the electrophoretic mobility of the polymers which make up the coating. We find that while not precisely the same, the two values are indeed comparable. Finally, we look at the role of varying the linear charge density of the polymers and compare this to experiments carried out by Danger et al., which examined how varying the amount of charge in a polyelectrolyte affects not only its electrophoretic properties but also the EOF produced by the polymer when used as a coating.[4]

II. THEORETICAL BACKGROUND

The simplest EOF is for the case of a flat charged surface with a no-slip boundary condition and with free counterions that are able to move with the fluid in response to an electric field parallel to the surface. At low Reynolds number, the governing relation is the Stokes equation with a driving force proportional to the electric field:

$$\nabla^2 v(h) = -\frac{E\rho(h)}{\eta} \tag{1}$$

where $v(h)$ is the velocity of the fluid at a height h above the wall, E is the electric field, $\rho(h)$ is the charge density at h, and η is the viscosity of the fluid. In the continuum limit, we can simply replace the charge density $\rho(h)$ with the Poisson equation yielding

$$\nabla^2 v(h) = -\frac{\epsilon E}{\eta}\nabla^2\phi(h) \tag{2}$$

where ϵ is the electric permittivity of the fluid and $\phi(h)$ is the potential at h. Integrating the above equation on both sides gives the well-known Helmholtz−Smoluchowski equation:

$$v_{\text{bulk}} = -\frac{\epsilon E\zeta}{\eta} \tag{3}$$

where v_{bulk} is the bulk solution velocity far from the wall and ζ is the zeta potential, the difference in the electrostatic potential of the bulk compared to where the liquid starts to shear near the surface. Often the bulk velocity is divided by the electric field in order to define the electro-osmotic mobility of the wall: $\mu_w \equiv v_{\text{bulk}}/E = \epsilon\zeta/\eta$. The zeta potential is often how surfaces are characterized in microfluidics although this concept is really only applicable to the case of uncoated capillaries.[19,20]

When the capillaries are coated by polymers the situation is remarkably different. For the case of uncharged polymer layers, the EOF is diminished due to the enhanced hydrodynamic drag between the moving fluid and the immobilized polymers. When the polymers are charged, on the other hand, they also contribute to the generation of EOF within the polymer layer due to the counterions associated with the charged groups on the polymers. The case of end-grafted polymers, polymers attached irreversibly by one end to a surface, has been extensively studied both experimentally and theoretically.[20]

For calculations of the EOF in the presence of surface grafted polymers, the scaling theory of Harden et al.,[13] for instance, provides predictions for the EOF far from a grafted polymer layer as a function of the degree of polymerization N, the grafting density γ, the electric field E, the free electrophoretic mobility of the polymers μ_p, and the electro-osmotic mobility of the bare wall μ_w. Thus, we discuss these predictions in some detail here in order to facilitate comparison with the simulation results of this paper.

The theoretical analysis of ref 13 considered the effects of grafted polymers on EOF in two regimes, namely the "mushroom" regime, where chains are sparsely grafted to the wall with little change in their equilibrium conformation, and the "brush" regime, where chains are grafted so densely that they tend to take on extended conformations due to the steric repulsion between adjacent chains. In the case of the mushroom regime in the low field limit, a simple scaling argument based on surface averaging of the EOF using the surface coverage of the polymer was predicted:

$$\mu_{\text{EOF}} = \mu_w - (\mu_w + \mu_p)(\gamma R_G^2) \qquad \text{for } \gamma R_G^2 < 1 \tag{4}$$

where $R_G \sim N^{3/5}$ is the (equilibrium) lateral radius of gyration of the polymers. In the "brush" regime of densely grafted polymers, the surface averaging approach is replaced with one based on transport in a porous polymer layer, which results in

$$\mu_{\text{EOF}} = -\mu_p + (\mu_w + \mu_p)\frac{1}{\cosh[(\gamma R_G^2)^{5/6}]} \tag{5}$$

In both cases, nonlinear terms related to the effect of the electric field E have been neglected, which is appropriate for the limit where the electric field is low. In this article we will examine both the scaling of the EOF mobility μ_{EOF} with respect to N and γ as well as the prediction of eqs 4 and 5 that the EOF goes from μ_w to $-\mu_p$ as N and γ increase.

III. SIMULATION MODEL

The model we use is based previous work by our group on neutral grafted polymer coatings.[7,8,21] We simulate EOF in a cylindrical tube with periodic boundary conditions along the axis of the tube. Simulations were conducted for both grafted and free polymers, the latter in order to measure their intrinsic electrophoretic mobility. The simulation's elements included beads representing neutral fluid, salt ions, monomers, and wall particles. All beads experience a purely repulsive WCA potential between each other:

$$\frac{U_{\text{WCA}}(r)}{\epsilon} = \begin{cases} 4\left[\left(\frac{\sigma_{\text{MD}}}{r}\right)^{12} - \left(\frac{\sigma_{\text{MD}}}{r}\right)^{6}\right] + 1 & r \le r_0 \\ 0 & r > r_0 \end{cases}$$

with $r_0 = 2^{1/6}\sigma_{\text{MD}}$. As is typical in MD simulations,[21] we choose $\varepsilon = k_BT$ as the fundamental MD energy scale and σ_{MD} as the fundamental MD length scale. The temperature is maintained via a dissipative particle dynamics thermostat (DPD).[22] Monomers of the polymer chains are linked to each other via FENE bonds: $U_{\text{FENE}}(r) = -0.5kR_0^2\ln[1-(r/R_0)^2]$, where $R_0 = 1.5\sigma_{\text{MD}}$ is the maximum extension of the bond and $k = 30\epsilon/\sigma_{\text{MD}}^2$ is the effective spring constant for the interaction. This potential is also used to bind the end of the polymer to the wall. Monomers are charged randomly until the desired average charge per monomer λ is attained. This is done by picking monomers randomly from all of the polymers in the system and not on a chain by chain basis. Thus, although the average charge per polymer is well-defined, the net charge is different for each polymer. This charging scheme was chosen in an effort to represent the experiments of Danger et al.[4] In their work they

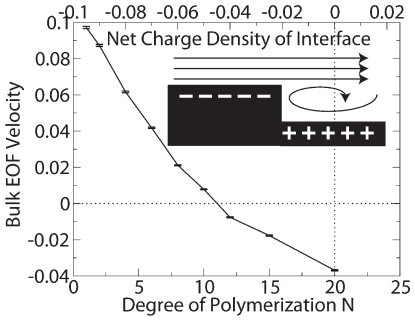

Figure 1. Average fluid velocity v_{EOF} within $2\sigma_{MD}$ of the center of the tube for the different values of N with $\gamma = 0.05$, $\lambda = 0.1$, $E = 3$, and $\sigma = -0.1$. The upper horizontal axis shows the effective interfacial charge density, $\sigma - \gamma\lambda N$, which is negative except for the last point where it is zero.

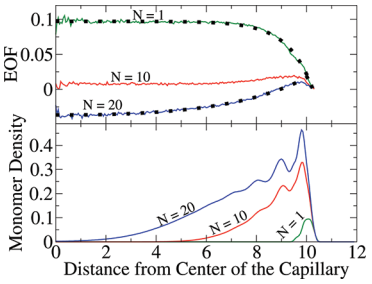

Figure 2. Fluid velocity and monomer density profiles as a function of r, the distance from the center of the capillary for $N = 1$ (green curves), $N = 10$ (red curves), and $N = 20$ (blue curves). The other simulation parameters are $\gamma = 0.05$, $\lambda = 0.1$, $E = 3$, and $\sigma = -0.1$ (the same as in Figure 1). The dotted lines (top panel) are fits, as described in the text.

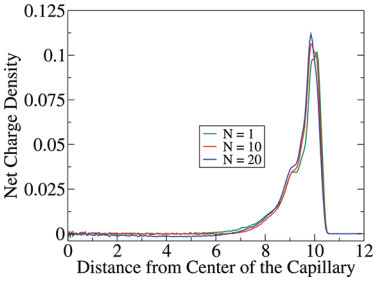

Figure 3. Net ion density (polymer and free ions) as a function of r, the distance from the center of the capillary for $N = 1$ (green curves), $N = 10$ (red curves), and $N = 20$ (blue curves). The other simulation parameters are $\gamma = 0.05$, $\lambda = 0.1$, $E = 3$, and $\sigma = -0.1$ (the same as in Figures 1 and 2).

synthesized heteropolymers made up of both charged and neutral monomers. As this is a common method of varying the linear charge density of polymers, we opted to use a similar methodology in our simulations. We also reserve two percent of the volume for positively and negatively charged fluid beads to create a strong ionic solution (this yields a Debye length of about $1\sigma_{MD}$[8,23]). In some simulations the wall beads are also charged randomly with σ charges per unit surface area. Additional fluid beads are charged in order to ensure that the whole system has a net charge of zero. Electrostatics are calculated using a Coulombic interaction with a cutoff of 1.5 times the diameter of the tube. The Bjerrum length was set to $2\sigma_{MD}$, an appropriate value for water.[8] Wall beads experience a harmonic potential about a point on an FCC lattice. Note that the wall beads have a mass $m_w = 3m$ while all the other beads have a mass of m (m is thus the MD mass scale). All numerical values given in this article are in terms of the fundamental energy, ε, length σ_{MD}, and mass m units of our MD simulations. The important parameters whose role we investigate are the degree of polymerization of the polymers, N, the polymer grafting density, γ (number of chains per unit surface area), the linear charge density of the polymers, λ (in units of e/monomer), the electric force, qE (in units of ϵ/σ_{MD} applied in the direction of the tube), and the wall charge σ (charge per unit surface area e/σ_{MD}^2). For a more detailed account of the method the reader is directed to a previous article on the simulation of neutral grafted polymer coatings.[8]

IV. RESULTS

A. Flow Reversal. In this section we examine how grafting positively charged polymers (linear charge density $\lambda = 0.1$) to a negatively charge surface ($\sigma = -0.1$) affects the EOF (fluid velocity) far from the surface. Interestingly, we find that the direction of the EOF reverses well before the net charge of the polymer−wall interface changes sign. This can clearly be seen in Figure 1, which shows the bulk EOF velocity v_{EOF} generated by a layer of polyelectrolyte chains grafted at fixed density as a function of their degree of polymerization, N. The net charge of the wall plus polymer coating for the last point on the x axis ($N = 20$) is actually zero, while the simulations involving shorter polymers all have an interface with a net negative charge. Despite this, the EOF clearly drops below zero for chains longer than $N = 10$. The physical cause of this flow reversal is that the EOF generated by the charges closer to the wall is more screened by the polymer layer than the EOF generated by those charges away from the wall. Thus, the EOF from charges localized on the wall is subject to the strongest quenching, while the EOF generated by charges along the grafted chains is progressively less screened as the free edge of the polymer layer is approached.

This surprising result has actually been seen in other electrokinetic systems. Polymers with both positive and negative monomers, but no net charge, in general have a nonzero mobility when subject to an electric field.[18,24] The reason for this is that the ends contribute more to the mobility since they tend to exist on the outside of the coil. In the context of EOF it was pointed out that a surface which undulates and has an equal number of positive and negative charges will tend to generate EOF in the direction of the charges which protrude farthest into the bulk.[25] A nice example of this is the use of three-dimensional electrodes to increase the EOF generated in induced-charge electro-osmosis (ICEO) as shown schematically in Figure 1. Using this concept, one can create a conveyor belt effect that dramatically increases EOF.[26]

Figure 2 shows the connection between the EOF and the density of polymers in the coating layer for chains of length $N = 1$, 10, and 20. The case of $N = 1$ corresponds to a nearly bare wall with a renormalized charge density. It is evident from the figure that there is a correlation between the radial variation of the EOF and the polymer density profiles due to a combination of polymer-induced EOF and hydrodynamic drag on the flow from the grafted polymer backbone. In particular, the magnitude of the fluid velocity changes where the monomer density is nonzero

dx.doi.org/10.1021/ma201995q |Macromolecules 2011, 44, 9455–9463

while it is constant near the center of the capillary where the monomer density is negligible. The situation is qualitatively different for the $N = 1$ case, where the counterions which make up the Debye layer actually extend beyond the end of the polymer layer and hence the fluid velocity reaches its plateau at the end of the Debye layer (near $r \approx 8$, as shown in Figure 3).

Figure 2 also shows fits to some of the data (the dotted lines). The fit for the fluid velocity profile of the $N = 1$ data has the form of a constant plug flow superimposed with an exponentially decaying flow

$$v_{EOF}(r) = v_{bulk}\left(1 - \exp\left[\frac{(-(R-r)}{\lambda_D}\right]\right) \quad (6)$$

where $\lambda_D = 1$ is the Debye length, v_{bulk} is the bulk EOF, and $R = 10.25$ is the radius of the capillary. This is the same profile as would be obtained for a simple Debye layer on a flat charged wall, which is a reasonable approximation given the large tube radius relative to the Debye length. The $N = 20$ data beyond the near wall region has been fit to the profile predicted by Harden et al.[13] for EOF flow past a charged surface with a uniform grafted polymer layer

$$v_{EOF}(r) = (\mu_p + \mu_w)\cosh\left[\frac{H-(R-r)}{d}\right] - \mu_p \quad (7)$$

where H is the mean height of the brush and $d \simeq \sigma^{-1/2}$ is the mean separation between grafted chains (both treated here as fitting parameters). The resulting values are $H = 9.78$, $d = 3.15$, $\mu_p = 0.042$, and $\mu_w = 0.022$, all of which are reasonable except for $\mu_w = 0.022$, which should be close to 0.1. The reason for this is that the parameter $\mu_p + \mu_w$ assumes that the velocity near the wall is still close to 0.1, the bare wall EOF velocity, though this is clearly not the case in Figure 2.

This form for the velocity profile within the brush has also been seen in MD simulations by Qiao and He for the case of neutral grafted chains.[10] From the $N = 20$ monomer density profile it is clear that the brush is nonuniform (unlike in the work of Harden et al. and Qiao and He, where the polymers formed a layer of constant density from the grafting surface to the edge of the brush). Nevertheless, the agreement of the fluid velocity profile with the theoretical prediction of Harden et al. is still quite good.

In Figure 3 we plot the net charge within the tube including the monomers and we see that except in the Debye layer near the wall the fluid is neutral. This means that the monomers' counterions are always nearby, making the system locally electrically neutral. This is necessary in order for the thin Debye layer approximation to be valid and the fluid velocity profile to obey eq 7.

B. Polymer Mobility. The theoretical expression for the bulk EOF in the presence of charged polymer coatings, eq 5, predicts that the flow generated by the charged wall is strongly screened in the case of sufficiently long polymers and that the EOF is only dependent on the electrophoretic mobility of the polymers, $\mu_{EOF} = -\mu_p$, in this limit. In order to test this prediction, we ran comparative simulations to determine the electrophoretic mobility of free polymers in solution.

The free solution electrophoresis simulations were carried out using the same model in the absence of a tube using the simulation package ESPResSo,[27] in order to avoid effects of confinement within the tube and correctly model long-ranged electrostatics with P3M. The EOF simulations were carried out

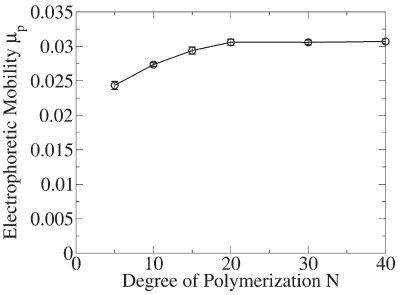

Figure 4. Electrophoretic polymer mobility μ_p as a function of chain length N of an isolated chain for $\lambda = 0.2$ and $E = 1$.

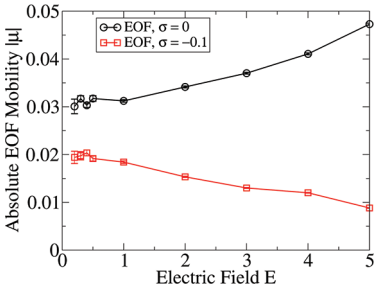

Figure 5. EOF mobility (both with and without wall charge) as a function of the electric field E for $N = 10$, $\gamma = 0.05$, and $\lambda = 0.2$.

in a confined geometry as described in a previous section. We first discuss the free-solution electrophoresis results. The data, shown in Figure 4, indicate an increase in the electrophoretic mobility of the polymers, μ_p, for short chains with a crossover to a constant mobility for sufficiently long chains, known as the free-draining limit. This is understood to be caused by the local balance of the electric driving force with the hydrodynamic friction caused by shearing of the fluid within the Debye layer.[16] We note that our data do not show some of the complex behavior found for short, highly charged chains in other recent simulations,[28,29] due to the low linear charge density λ which minimizes counterion condensation effects (note that the Bjerrum length was set at 2 while the charge density along the polymer was $\lambda = 0.2$).

Turning to the EOF simulations, we note that the relationship between bulk EOF in the presence of polymer coatings and the applied electric field is highly nonlinear at high electric fields. This has important implications for the effective mobility of the polymers in the grafted layer. In the case of neutral chains, the nonlinear response is caused by the stretching of the chains in the direction of the flow, which causes a reduction in the coating's height and thus increases the EOF.[10−13,30] As we shall see, the physics is much more complicated in the case of charged chains where there is both a reduction in coating height and increased electrophoretic mobility of the polymers comprising the coating as they align with the electric field.

Figure 5 shows the effective EOF mobility in the presence of charged grafted polymers as a function of the electric field E (for $N = 10$, $\lambda = 0.2$, and $\gamma = 0.05$), both with and without wall charges. For low electric fields we see that the EOF mobility appears to be fairly constant both with and without wall charges. As the field increases, however, the EOF mobility in the absence of wall charge increases, due to the deformation and alignment of the chains with the electric field, which becomes large around

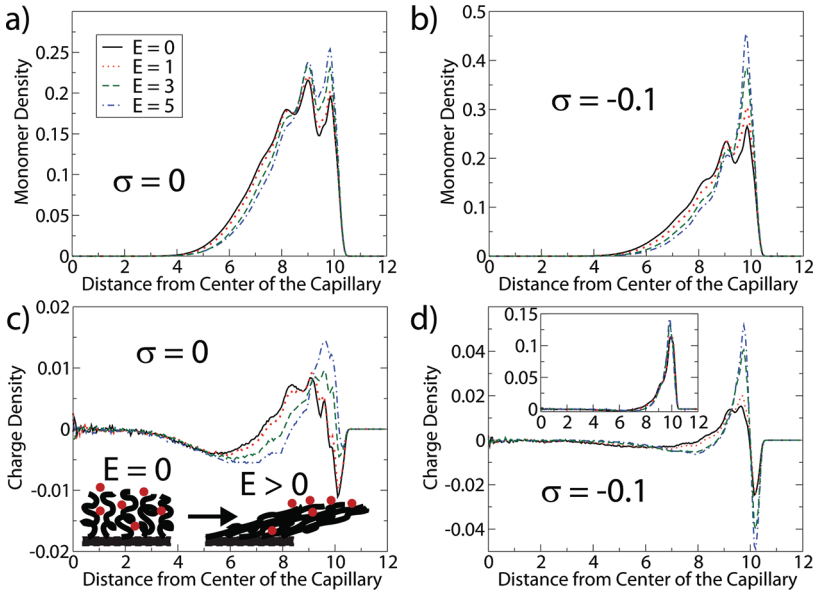

Figure 6. Radial monomer density profiles are shown for uncharged walls (a) and charged walls (b) at various values of the electric field E. Below the monomer density profiles are the radial charge density profiles again for uncharge walls (c) and charged walls (d). The inset in (d) is the charge density profile before subtracting off the charge density profile of a bare tube with the same wall charge. All simulations are done with $N = 10$, $\gamma = 0.05$, and $\lambda = 0.2$.

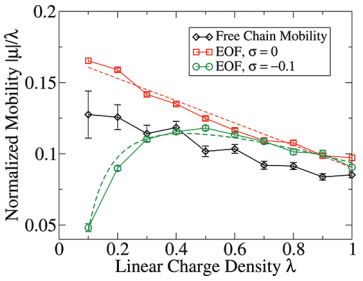

Figure 7. Effect of varying the linear charge density, λ, along the polymer backbone for $N = 10$, $\gamma = 0.05$ (for the two EOF cases), and $E = 1$. The results for EOF with and without a wall charge σ as well as the polymer's free-solution electrophoretic mobility are shown. All mobility values are renormalized by λ. The dashed lines are fits to the data, as described in the text. Note that the flow generated by the bare wall for the $\sigma = -0.1$ case would actually be in the opposite direction.

$E = 1$, and the concomitant change in the charge density profile away from the grafting wall, as seen in Figure 6a,c. Mobile negative charges are squeezed out of the collapsing polymer layer, leading to a contribution to the EOF that is not screened by the polymer layer. This effect is schematically illustrated in Figure 6c. Another possible mechanism for this increase in EOF is the increase in the mobility of the polyelectrolytes, μ_p, as the electric field causes the polymers to align with the electric field.[31,32]

The nonlinear behavior is different for the case of charged walls ($\sigma = -0.1$) where the electro-osmotic mobility of the polymer−wall interface decreases with increasing electric field. In this case, the wall charge produces a flow in the direction of the field (which is the opposite direction of the net EOF caused by the polymers). This fluid flow causes hydrodynamic drag on the polymers along the capillary axis which helps to stretch the chains which are being pulled by both the electric field and the wall's EOF. This leads in turn to the coating being less effective in screening the flow caused by the wall charges, due to a reduction in its height. The increased effect of the wall charge in this instance appears to dominate over the effects of the polymer layer conformation on the distribution of the mobile charges, as can be seen in Figure 6b,d. Since nonlinear effects due to the electric field become significant for $E > 1$, we use $E = 1$ in the rest of the article to study the simplest case.

C. Varying the Linear Charge Density. Next the effect on the mobility of varying the linear charge density, λ, on the backbone of the polymer was investigated for both free and grafted chains. Figure 7 shows the ratio $|\mu|/\lambda$ as a function of λ for $E = 1$, $N = 10$, and $\gamma = 0.05$ (for the grafted chains). Clearly, for all values of λ, the EOF mobility is slightly higher than the electrophoretic mobility in the case of an uncharged ($\sigma = 0$) wall although the two curves slowly converge. In the case of a charged wall ($\sigma = -0.1$), however, we see that at first the electrophoretic mobility is much higher than the EOF. This is because the parameters chosen for the grafted polymer coating are such that the flow caused by the wall charges is not entirely screened by the polymer coating. For sufficiently large λ, however, the influence of the polymer charges overwhelms that of the wall charges, and the normalized mobility values tend to converge for EOF in both cases. Figure 7 shows a crossover to polymer charge dominance at approximately $\lambda = 0.4$. In the large λ limit, the electrophoretic mobility is always smaller than the EOF mobility for both charged and uncharged walls.

These results are similar to the experimental results reported by Danger et al.,[4] which compared the EOF and electrophoretic mobilities for heteropolymers with different net charges. For the experimental EOF measurements, the polymer coatings were composed of successively adsorbed polyelectrolyte layers, a situation that is qualitatively similar to having an underlying wall charge below a diffuse polymer layer. Contrary to the simulations, the electrophoretic mobility was found experimentally to be large compared to the effective EOF mobility for weakly charged chains. However, this difference became smaller with increasing charge on the polymer. These differences at small

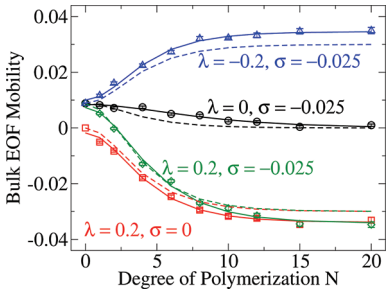

Figure 8. Bulk EOF mobility as a function of the polymer length N for $\gamma = 0.05$ and $E = 1$. The graph shows four different cases: neutral polymers, $\lambda = 0$, with wall charge $\sigma = -0.025$ (black circles); positively charged polymers, $\lambda = 0.2$, without wall charge (red squares) and with wall charge $\sigma = -0.025$ (green diamonds); and negatively charged polymers, $\lambda = -0.2$, with wall charge $\sigma = -0.025$ (blue triangles). The solid lines are best fits to the data using the functional form of eq 5 while the dashed lines use eq 5 with the theoretical parameters from Table 1.

λ between our simulations and the experiments could be due to differences in the stability between the physically adsorbed polymer layers of the experiments in comparison with the irreversibly grafted polymers considered by the simulations. In particular, Danger et al. hypothesized that the observed EOF was much lower than the electrophoretic mobility at low λ due to weak adsorption of charged polymers at low λ, leading to incomplete, patchy coverage of the surface. Although, as noted below, there are other equally plausible explanations.

For the $\sigma = 0$ simulation data, the scaled mobility appears to be a roughly linear function of λ, implying that $\mu_{EOF}/\lambda \approx C_0 - C_1\lambda$. The fit to this form (the dashed red line in the figure) for $\sigma = 0$ yields $C_0 = 0.17$ and $C_1 = -0.078$. More generally, in the presence of both polymer and wall charge, eqs 4 and 5 can be rewritten in a generic form: $\mu_{EOF} = A\mu_w + B\mu_p$ where A and B are constants that depend only on γR_G^2 (the height and density of the polymer layer). Substituting $\mu_p/\lambda \approx C_0 - C_1\lambda$ yields $\mu_{EOF} = A\mu_w + B\lambda(C_0 - C_1\lambda)$. This implies that the correct fit to the simulation data for the case where the wall charge is $\sigma = -0.1$ should have an additional term A/λ, $\mu_{EOF}/\lambda \approx A/\lambda + C_0 + C_1\lambda$, as long as the polymer brush conformation is unaffected by λ (a reasonable assumption for weak-to-moderate charging and small-to-moderate Debye lengths). For the particular case of $\sigma = -0.1$ shown in Figure 7, the best fit values are $C_0 = 0.17$, $C_1 = -0.063$, and $A = -0.116$ (the dashed green line in the figure). This result suggests an alternative to the explanation proposed by Danger et al. for the relatively small EOF mobility at small λ compared to the free solution electrophoretic mobility, namely the incomplete screening of the wall charge contribution to the EOF by the underlying polyelectrolyte layers. While this does not refute the hypothesis put forth by Danger et al. that there is incomplete surface coverage of the last layer, it suggests that the results might in fact simply be due to an incomplete screening of the EOF caused by the underlying polyelectrolyte layers.

We note that all three of the curves for μ/λ in Figure 7 have a downward slope at high λ. This reduced mobility, compared to what one might intuitively expect—a constant ratio of μ to λ reflecting a simple linear increase of μ with respect to λ—may be due to the condensation of counterions onto the backbone.[33] This phenomenon has been seen in other simulations of electrophoresis[28,29] and also in the work of Danger et al.[4]

Table 1. Fitting Parameters for Figure 8 Using eq 5[a]

	fit parameters		
set	μ_p	μ_w	H_0
$\lambda = 0$, $\sigma = -0.025$	−0.000 11	0.0087	5.1
$\lambda = 0$, $\sigma = -0.025$ theory	0	0.0088	8.7
$\lambda = 0.2$, $\sigma = 0$	0.034	−0.0018	9.9
$\lambda = 0.2$, $\sigma = 0$ theory	0.030	0	8.7
$\lambda = 0.2$, $\sigma = -0.0250$	0.034	0.0073	8.9
$\lambda = 0.2$, $\sigma = -0.0250$ theory	0.030	0.0088	8.7
$\lambda = -0.2$, $\sigma = -0.0250$	−0.035	0.010	10.1
$\lambda = -0.2$, $\sigma = -0.0250$ theory	−0.030	0.0088	8.7

[a] Both theoretical values (for the dashed lines) and best fit values (for the solid lines) are given.

There may also be other sources of nonlinear response at large λ. This behavior could be induced by osmotic swelling of the polyelectrolyte layers, a well-known effect for grafted polyelectrolytes which we also see in our simulations for the highest values of λ (data not shown). Such nonlinear effects, while fascinating, are beyond the scope of this work. In the following, we chose to focus on the relatively small value of $\lambda = 0.2$, where such nonlinear behavior is not dominant.

D. Varying the Polymer Length. The results given in Figure 8 show in a systematic way how increasing the polymer length N affects the bulk EOF. The most basic case is that of a neutral polymer $\lambda = 0$ and a charged wall $\sigma = -0.025$ (black circles), a case previously studied using the same simulation method in our group.[7,8] The results in this limit agree with the scaling arguments of Harden et al.[8,13] Initially, the bulk EOF is determined by the electroosmotic mobility of the wall μ_w, but as the chain length increases, the EOF approaches zero asymptotically according to eq 5.

Slightly more complicated is the case of charged chains ($\lambda = 0.2$) grafted on an uncharged wall ($\sigma = 0$), represented by the red squares in Figure 8 . In the limit $N \to 0$, the EOF largely determined by the electroosmotic mobility of the wall μ_w, which in this case is zero. With increasing N, the EOF approaches a value which is related to the electrophoretic mobility of a polymer chain, μ_p. In the limit of infinitely thin Debye layer and polymer backbone, the EOF mobility is predicted to be given by $\mu_{EOF} = -\mu_p = 0.03$ (from Figure 4) for sufficiently thick polymer layers.[13]

For the case of a charged polymer $\lambda = 0.2$ with an oppositely charged wall $\sigma = -0.025$ (the green diamonds in Figure 8), we see both effects. With increasing polymer length, the flow generated by the wall charges is not only quenched, but the flow generated by the counterions of the polymer coating becomes increasingly dominant. Consequently, for an increasingly thick polymer layer the bulk EOF is less and less dependent on the properties of the wall, μ_w, and more and more dependent on the properties of the polymer coating, μ_p, as previously predicted.[13]

The last curve shows the case of a negatively charged polymer $\lambda = -0.2$ on a negatively charged wall $\sigma = -0.025$ (blue triangles in Figure 8), where the EOF is much less dependent on the thickness of the polymer coating. This is because the EOF induced slip along the backbone of the polymer is similar to the electroosmotic mobility of the charged wall. Note that the value this curve approaches for large values of N is simply the

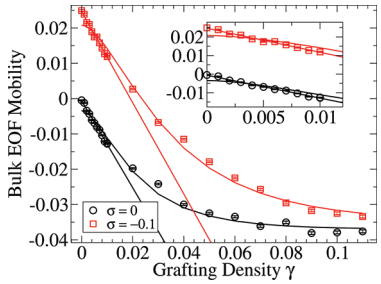

Figure 9. Effect of varying the grafting density, γ, of the polymer coating on the EOF for $N = 10$, $\lambda = 0.2$, and $E = 1$ in the case of a charged ($\sigma = -0.1$) and uncharged ($\sigma = 0$) wall. The inset shows a closeup of the region near $\gamma = 0$. The straight lines are the fits for the mushroom regime, eq 4, while the curved lines are fits for the brush regime, eq 8.

Table 2. Fitting Parameters for Figure 9 Using eq 8[a]

	fit parameters		
set	μ_p	μ_w	H_0
$\sigma = 0$	−0.037	0.0034	8.58
$\sigma = 0$ theory	−0.030	0	8.05
$\sigma = -0.1$	−0.035	0.021	5.85
$\sigma = -0.1$ theory	−0.030	0.025	8.05

[a] Both theoretical values and best fit values are given here while the graph shows only the curves for the best fit parameters.

opposite of the value of the two positively charged $\lambda = 0.2$ coatings, as expected.

For all of the curves we have successfully fit the data with eq 5, using μ_p, μ_w, and a numerical prefactor H_0 in the argument of the cosh as fitting parameters, given in Table 1. We also use the hydrodynamic radius R_H in place of the radius of gyration R_G as this has previously been shown to be the relevant quantity.[8] With the addition of the of the numerical prefactor H_0, eq 5 becomes

$$\mu_{EOF} = -\mu_p + (\mu_w + \mu_p)\frac{1}{\cosh[H_0(\gamma R_H^2)^{5/6}]} \quad (8)$$

The fitting values of these parameters can be compared with theoretical estimates. The theoretical value of $\mu_w = 0.0088$ given in the table is the bulk EOF generated in a simulation by a capillary with a wall charge of $\sigma = -0.025$ and no polymer coating, while the theoretical value of $\mu_p = 0.03$ is the asymptotic long chain mobility taken from Figure 4 . We estimate the value for H_0, the unspecified constant in the scaling expression for the height of the brush, eq 5, by imposing equality of the volume per grafted chain in the mushroom and brush regime at the crossover from mushroom to brush. In the mushroom regime, the volume is simply given by $V = MV_i = M(4/3\pi R_H^3)$ where M is the number of grafted polymers and V_i is the volume of each individual polymer. In the brush regime, the volume of the coating is $V = MV_i = MH/\gamma$, where the height of the brush is given by $H = H_0(\gamma R_H^2)^{5/6}$.[13] Setting these two volumes equal yields $H_0 = (4/3\pi R_H^3)\gamma/(\gamma R_H^2)^{5/6})$, where R_H is chosen as the value which satisfies $\pi\gamma R_H^2 = 1$, a value we have previously identified as a reasonable condition for the crossover from mushroom to brush behavior.[8]

Overall, the tabulated results for the theoretical values and the best fits for these three parameters are in fairly good agreement, as can be seen by comparing the two curves in Figure 8 generated by theoretical values (dashed lines) and the fit values (solid lines). The value of μ_w appears to be within about 20% of the expected value for all four curves. The value representing the free solution polymer mobility, μ_p, is very close for the three charged coatings. Interestingly, however, it is systematically higher than the theoretical value, which we ascribe to the finite extent of our Debye layer as described in more detail in the next section. The value of H_0 is also systematically higher than we expect, although it is within about 10% for the three cases where $\lambda \neq 0$. The fit for $\lambda = 0$, $\sigma = -0.025$ shows a value of H_0 which is about half as large as for the charged polymer coatings. We believe that this is because the charged brushes have an effective volume which incorporates not only the hydrodynamic radius, R_H, but also the Debye length, λ_D, giving them an effective hydrodynamic radius of $R_H + \lambda_D$. We will show further evidence for this in the next section which looks at the effect of the grafting density.

E. Varying the Grafting Density. In this section we investigate the validity of the scaling predictions for the EOF given in eqs 4 and 5 with respect to the grafting density γ. The results are summarized in Figure 9 and Table 2. For small values of γ (the sparsely grafted mushroom regime), we expect to see a roughly linear relationship between the EOF and γ, as predicted by eq 4. Such linear behavior does appear for $\gamma \leq 0.01$; however, the mushroom regime behavior clearly ends well before the expected crossover to brushlike behavior at $\gamma = 1/\pi R_H^2 \approx 0.059$. The best fit slopes to the MD data for $\gamma \leq 0.01$ are −1.29 and −1.23 for the cases of a charged wall ($\sigma = -0.1$) and an uncharged wall ($\sigma = 0$), respectively.

The values of the slopes in the low density regime are significantly different than those expected theoretically. According to Harden et al.[13] and based on the results of Tessier and Slater,[8] we would expect a slope of approximately $-\pi R_H^2(\mu_w + \mu_p)$. Using an estimate for the bare hydrodynamic radius based on simulation data, we obtain $R_H \sim 2.2R_G \simeq 3.4$. In the case of the charged wall ($\sigma = -0.1$) this yields a slope of roughly −1, while for the uncharged wall ($\sigma = 0$) we obtain a slope of roughly −0.58. Thus, for both cases, there is a small deviation between the theoretically predicted and the observed slopes. One important difference between our simulation studies and the theoretical model is the finite value of the Debye length. Whereas the theoretical expressions are strictly only valid in the limit of an arbitrarily thin Debye layer around a structureless polymer backbone, our simulations consider a Debye length of $\lambda_D \approx 1$. This finite Debye length may contribute to a larger effective hydrodynamic radius. Interestingly, if we use a slightly modified expression for the slope that accounts for this increase in the effective hydrodynamic radius, $\pi(R_H + \lambda_D)^2(\mu_p) \approx 1.22$, we obtain a value which is quite close to the observed results for the case of the uncharged wall ($\mu_w = 0$). This value is also serendipitously close to the fitted value for the case of the charged surface as well, whereas one might expect that the value for the charged wall to be about twice as large, according to eq 4. The lack of difference between the charged and uncharged slope values may be due to a redistribution of the wall's counterions into the interstitial space between the sparsely grafted chains, thereby diminishing the μ_w dependence of the slope in the "mushroom" regime. We note, however, that this effect disappears in the more densely grafted limit.

For higher values of γ (the brush regime; $\gamma \gg 0.1$), the dependence of the EOF on γ takes the form of a hyperbolic cosine, eq 8, with a magnitude that asymptotically approaches μ_p,

the electrophoretic mobility of the polymers which make up the coating. We fit the data (solid lines in Figure 9) using eq 8; the fit values are given in Table 2 along with theoretical predictions based on ref 13. The resulting values for μ_w and H_0 in Table 2 are in fair agreement with their theoretical counterparts, much like was seen in Table 1 and Figure 8 . However, it is notable that the simulation values of the EOF at large values of γ significantly exceed the corresponding electrophoretic mobility of polymers with a linear charge density $\lambda = 0.2$, $\mu_p \approx 0.30$.

This is reminiscent of behavior seen in Figure 8 in the previous section and is suggestive of the influence of finite Debye length on the densely grafted polymers. In particular, the Debye length of our MD simulations, $\lambda_D = 1$, is comparable to the average distance between adjacent polymers at the higher grafting densities we have simulated, indicating significant overlap of Debye layers of adjacent grafted polyelectrolyte chains. In nanoscopic systems it is well-known that there must be corrections to classical theory due to overlapping Debye layers.[23,34] In this case, the overlap of the Debye layers of adjacent polyelectrolytes leads to an increase of the electro-osmotic mobility of the coating beyond the electrophoretic mobility of the individual polymers due to the reduction in screening. This is the same effect that causes the initial increase in Figure 4 for the polymer mobility as a function of N.[16,28,29] Similar results have also been observed in the electrophoresis of colloids in the low salt regime where the mobility was found to increase with increasing packing fraction in the very low concentation regime.

V. CONCLUSION

In this article we presented simulation results addressing the role of charged polymer coatings in the modulation of EOF. In particular, we focused on the case of grafted polymer coatings. We believe that the results found in our simulations are also relevant to the more common experimental practice of adsorbed, charged polymer coatings as we showed with our comparison to the experimental results of Danger et al.[4] Our results show a strong similarity between successively adsorbed ionic coatings and our simulations of an ionic polymer coating grafted onto an oppositely charged wall. We attempted to compare our results to the theoretical predictions of Harden et al.,[13] and we were able to establish evidence that there is a linear relationship between the EOF and the grafting density γ in the case of the mushroom regime. We also found good agreement with the scaling predictions both as a function of grafting density γ and degree of polymerization N for the brush regime.

One small difference between the results of our MD simulations and the theoretical predictions of Harden et al.[13] is that we find EOF values which are somewhat larger than the electrophoretic mobility of the same polymers. The theoretical calculations of Harden et al.[13] were based on the assumption that the Debye layer is infinitely thin and an infinitely thin polymer backbone, and we hypothesize that the fact that these assumptions are not true in the case of our simulations is the reason for $\mu_{EOF} > \mu_p$.

While our results focus on the role of polyelectrolytes grafted to a solid surface on EOF, they are also be applicable to the electrophoresis of a colloid grafted with a polyelectrolyte.[19,36−40] Essentially, the difference between the bulk fluid velocity and the stationary wall is governed by the same phenomena as the eletrophoretic speed of these soft colloids. In fact, one of the first studies on the electrokinetic effects of polyelectrolytes grafted to a surface focuses on understanding the electrophoretic behavior of human erythrocyte cells.[41] The electrophoretic results indicated that the glycocalyx which coated the cell's surface acted essentially as a polyelectrolyte coating. The electrophoresis of cells is still often understood within this context.[42,43]

AUTHOR INFORMATION

Corresponding Author

*E-mail: gary.slater@uOttawa.ca.

ACKNOWLEDGMENT

We thank Mark D. Whitmore for helpful discussions. This work was supported by NSERC Discovery grants to G.W.S. and J.L.H. C.H. thanks the Volkswagen foundation and the DFG through SimTech and the SFB 716 for financial support. O.A.H. also acknowledges funding from a University of Ottawa Entrance Scholarship and NSERC through the CGS and Michael Smith programs. Sharcnet provided computational resources for this work.

REFERENCES

(1) Long, D.; Stone, H. A.; Ajdari, A. *J. Colloid Interface Sci.* **1999**, *212*, 338.
(2) Doherty, E. A. S.; Meagher, R. J.; Albarghouthi, M. N.; Barron, A. E. *Electrophoresis* **2003**, *24*, 34.
(3) Znaleziona, J.; Petr, J.; Knob, R.; Maier, V.; Ševčík, J. *Chromatographia* **2008**, *67*, 5.
(4) Danger, G.; Ramonda, M.; Cottet, H. *Electrophoresis* **2007**, *28*, 925.
(5) Lazar, I. M.; Karger, B. L. *Anal. Chem.* **2002**, *74*, 6259.
(6) Gregersen, M. M.; Okkels, F.; Bazant, M. Z.; Bruus, H. *New J. Phys.* **2009**, *11*, 075019.
(7) Tessier, F.; Slater, G. W. *Macromolecules* **2005**, *38*, 6752.
(8) Tessier, F.; Slater, G. W. *Macromolecules* **2006**, *39*, 1250.
(9) Qiao, R. *Langmuir* **2006**, *22*, 7096.
(10) Qiao, R.; He, P. *Langmuir* **2007**, *23*, 5810.
(11) Cao, Q.; Zuo, C.; Li, L.; Ma, Y.; Li, N. *Microfluid. Nanofluid.* **2010**, 1.
(12) Cao, Q.; Zuo, C.; Li, L.; Yang, Y.; Li, N. *Microfluid. Nanofluid.* **2010**, 1.
(13) Harden, J. L.; Long, D.; Ajdari, A. *Langmuir* **2001**, *17*, 705.
(14) Hickey, O. A.; Harden, J. L.; Slater, G. W. *Phys. Rev. Lett.* **2009**, *102*, 108304.
(15) Doherty, E. A. S.; Berglund, K. D.; Buchholz, B. A.; Kourkine, I. V.; Przybycien, T. M.; Tilton, R. D.; Barron, A. E. *Electrophoresis* **2002**, *23*, 2766.
(16) Shendruk, T. N.; Hickey, O. A.; Slater, G. W.; Harden, J. L. *Curr. Opin. Colloid Interface Sci.* **2011**, DOI: 10.1016/j.cocis.2011.08.002.
(17) Long, D.; Viovy, J. L.; Ajdari, A. *Phys. Rev. Lett.* **1996**, *76*, 3858.
(18) Hickey, O. A.; Holm, C.; Harden, J. L.; Slater, G. W. *Phys. Rev. Lett.* **2010**, *105*, 148301.
(19) Dukhin, S. S.; Zimmermann, R.; Duval, J. F. L.; Werner, C. *J. Colloid Interface Sci.* **2010**, *350*, 1.
(20) Duval, J. F. L.; Gaboriaud, F. *Curr. Opin. Colloid Interface Sci.* **2010**, *15*, 184.
(21) Slater, G. W.; Holm, C.; Chubynsky, M. V.; de Haan, H. W.; Dube, A.; Grass, K.; Hickey, O. A.; Kingsburry, C.; Sean, D.; Shendruk, T. N.; Zhan, L. *Electrophoresis* **2009**, *30*, 792.
(22) Soddemann, T.; Düunweg, B.; Kremer, K. *Phys. Rev. E* **2003**, *68*, 46702.
(23) Tessier, F.; Slater, G. W. *Electrophoresis* **2006**, *27*, 686.
(24) Long, D.; Dobrynin, A. V.; Rubinstein, M.; Ajdari, A. *J. Chem. Phys.* **1998**, *108*, 1234.
(25) Ajdari, A. *Phys. Rev. E* **1996**, *53*, 4996.
(26) Bazant, M. Z.; Ben, Y. *Lab Chip* **2006**, *6*, 1455.

(27) Limbach, H. J.; Arnold, A.; Mann, B. A.; Holm, C. *Comput. Phys. Commun.* **2006**, *174*, 704.
(28) Grass, K.; Böhme, U.; Scheler, U.; Cottet, H.; Holm, C. *Phys. Rev. Lett.* **2008**, *100*, 96104.
(29) Frank, S.; Winkler, R. G. *Europhys. Lett.* **2008**, *83*, 38004.
(30) Cohen, Y.; Metzner, A. B. *Macromolecules* **1982**, *15*, 1425.
(31) Stigter, D.; Bustamante, C. *Biophys. J.* **1998**, *75*, 1197.
(32) Long, D.; Viovy, J. L.; Ajdari, A. *Biopolymers* **1996**, *39*, 755.
(33) Manning, G. S. *J. Chem. Phys.* **1969**, *51*, 3249.
(34) Huang, K. D.; Yang, R. J. *Nanotechnology* **2007**, *18*, 115701.
(35) Palberg, T.; Medebach, M.; Garbow, N.; Evers, M.; Fontecha, A. B.; Reiber, H.; Bartsch, E. *J. Phys.: Condens. Matter* **2004**, *16*, S4039.
(36) Duval, J. F. L.; van Leeuwen, H. P. *Langmuir* **2004**, *20*, 10324.
(37) Ohshima, H. *Colloid Polym. Sci.* **2007**, *285*, 1411.
(38) Hsu, J. P.; Chen, Z. S.; Tseng, S. *J. Phys. Chem. B* **2009**, *113*, 7701.
(39) Dukhin, S. S.; Zimmermann, R.; Werner, C. *J. Colloid Interface Sci.* **2007**, *313*, 676.
(40) Dukhin, S. S.; Zimmermann, R.; Werner, C. *Adv. Colloid Interface Sci.* **2006**, *122*, 93.
(41) Levine, S.; Levine, M.; Sharp, K. A.; Brooks, D. E. *Biophys. J.* **1983**, *42*, 127.
(42) Lokar, M.; Urbanija, J.; Frank, M.; Hägerstrand, H.; Rozman, B.; Bobrowska-Hägerstrand, M.; Iglic, A.; Kralj-Iglic, V. *Bioelectrochemistry* **2008**, *73*, 110.
(43) Hyono, A.; Gaboriaud, F.; Mazda, T.; Takata, Y.; Ohshima, H.; Duval, J. F. L. *Langmuir* **2009**, *25*, 10873.